J. Fluid Mech. (1984), *vol.* 139, *pp.* 173–191
Printed in Great Britain

Hydrodynamics of small tubular pumps

By J. F. DIJKSMAN
Philips' Research Laboratories, P.O. Box 80.000, 5600 JA Eindhoven, The Netherlands

(Received 30 June 1982 and in revised form 12 September 1983)

Miniature tubular pumps are used to emit droplets from ink-jet matrix heads. This paper deals with the simulation of the behaviour of a viscous and compressible liquid in such pumps. The response of the liquid in the frequency and time domain is analysed.

An approximate method is given to determine the droplet speed and size.

1. Introduction

Miniature tubular pumps are used as the droplet-emitting parts in devices, such as ink-jet matrix heads, that work according to the droplet-on-demand principle.

Each pump of such a head consists of a glass tube which is partly surrounded by a thick-walled tube made of radially polarized piezoelectric ceramic material (Berlincourt, Curran & Jaffe 1964; Philips 1974). One end of the glass tube is connected to the reservoir, for instance by a tube with a relatively small cross-section, the purposes of which are damping and avoiding cross-talk. The other end is a nozzle. Characteristic data of such a pump are:

overall length 30–50 mm;
inside diameter 0.4–1 mm;
nozzle diameter about 0.1 mm;
wall thickness of glass tube about 0.05 mm.

The action of a pump working according to the droplet-on-demand principle is broadly as follows. Owing to a sudden volume change caused by a pulsewise voltage change across the piezoceramic tube, pressure waves are built up, which start travelling through the glass tube. At the moment that a positive pressure wave hits the nozzle, the fluid there will be pushed outwards. When the amount of kinetic energy transferred outwards is larger than the surface energy needed to form a droplet, a droplet can in principle be launched. Whether in reality a droplet is released and what its velocity is will depend on the amount of kinetic energy transferred outwards in excess of the surface energy needed to form a droplet. In order to overcome the decelerating action of the ambient air, the droplet must have an initial velocity of several metres per second. The pulse height is chosen in such a way that just one droplet is formed. By damping, the next positive-pressure waves that arrive at the nozzle must be made so small that no droplet is launched until the piezoceramic actuator is charged again.

In §2 an approximate theory is presented, which makes it possible to predict the response of miniature tubular pumps in both the frequency domain and the time domain, including the effects of the geometry of the pump, the shape of the charge pulse and the physical properties of the ink, such as its viscosity, compressibility and density.

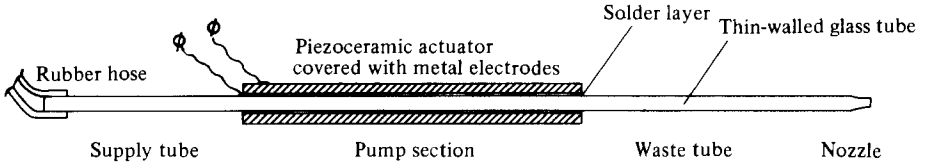

FIGURE 1. Schematic set-up of a miniature tubular pump.

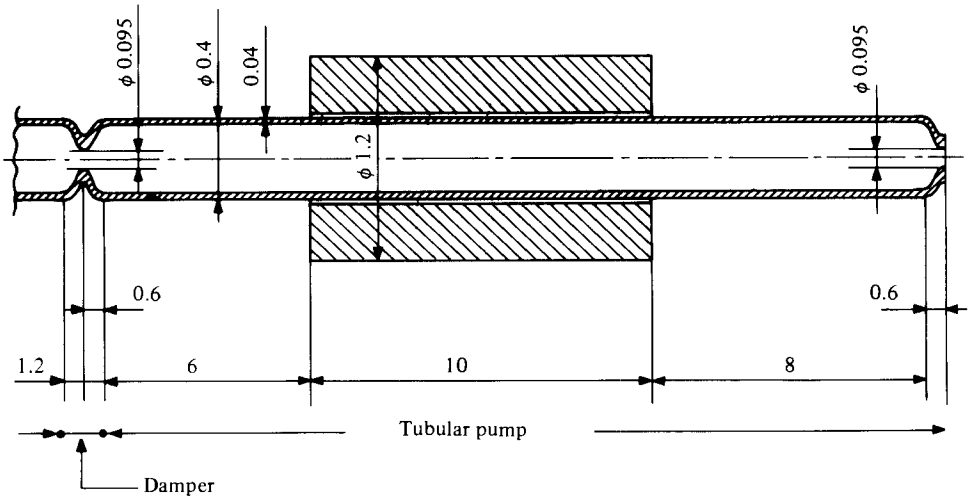

FIGURE 2. Example of a miniature tubular pump (all dimensions in mm). In the drawing the cross-sectional dimensions are enlarged by a factor of 5 with respect to the length. Glass tube: wall thickness 0.04 mm, Young's modulus 6.4×10^{10} Pa. Actuator: material PZT-5 (Berlincourt *et al.* 1964), radial displacement inside 0.26×10^{-4} mm/100 V, lowest longitudinal resonance frequency 200 kHz. Fluid: ethylene glycol: $\mu = 0.02$ Pa s, $\sigma = 0.05$ N/m, $\rho = 1113$ kg/m^3, $c = 1680$ m/s (Weast 1974).

Section 3 deals with a method that can be used to predict the droplet size and the droplet speed. The droplet formation is highly dependent on the surface tension of the ink.

2. Analysis of pump action

Consider the geometry shown in figure 1. The frame of reference is a cylindrical coordinate system (r', θ', z'). The z' axis lies along the centreline of the pump, which may be slightly curved (e.g. for integration in a multinozzle print head). Its positive direction equals the direction of the net flow through the pump. The lines $r' =$ constant and $\theta' =$ constant are in the circumferential and radial directions respectively. The motion of the ink, which has constant properties, is axisymmetric with respect to the z'-axis. During action the temperature remains constant.

The analysis proceeds as follows. The pump is divided into several parts in such a way that each part is a circular cylindrical tube with constant properties and cross-sectional dimensions. Apart from a set of constants, the behaviour of the fluid contained in such a part can be calculated. The sets of constants can be found by using the conditions at the end and the beginning of the pump and by evaluating the compatibility conditions between the parts. A typical example of a tubular pump

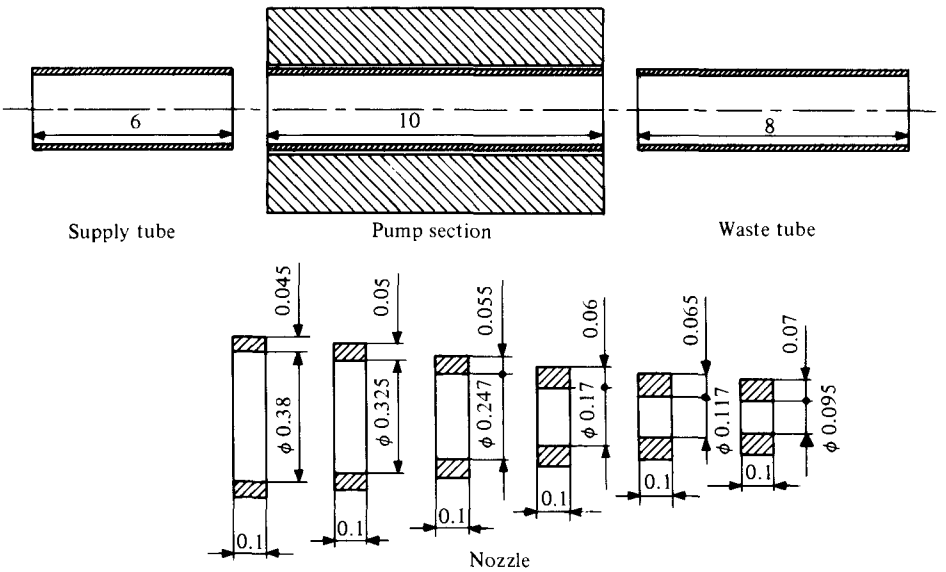

FIGURE 3. Division into elements (all dimensions in mm). The damper consists of two nozzle-shaped parts.

is shown in figure 2. Figure 3 gives an overview of the division of this pump into the parts described earlier.

We start with the analysis of the pump in the frequency domain. After that we can calculate by Fourier analysis the response of the system in the time domain.

First, we make some preliminary remarks. An estimate of the pressures induced in the pump by applying a voltage of 100 V across the actuator, which is a representative value, can be arrived at by the following reasoning (see data of figure 2). It is assumed that the radial displacement of the inside of the piezoceramic tube and the radial displacement of the inside of the glass tube which it surrounds are equal. Consider the case that the inside of the glass tube is moved stepwise inward over a distance equal to 0.26×10^{-4} mm. This step is generated so fast that the displacement of the fluid in the axial direction is negligible. This is true because the velocity is limited by the velocity of sound and the tube is long relative to its diameter. Then the pressure rise inside the pump section can be calculated as

$$\Delta p = -K\Delta V/V, \tag{1}$$

where K is the compression modulus of the fluid, which is related to the velocity of sound by

$$c = (K/\rho)^{\frac{1}{2}}. \tag{2}$$

Inserting $R = 0.2$ mm and $K = 3 \times 10^9$ Pa (ethylene glycol) we find $\Delta p \approx 7 \times 10^5$ Pa. This value may be expected to be representative of the maximum value of the pressure waves travelling through the system.

The displacement w for a glass tube with inner radius $R = 0.2$ mm, wall thickness $h = 0.04$ mm and Young's modulus $E = 6.4 \times 10^{10}$ Pa loaded by an inside pressure of 7 bar is roughly equal to 10^{-5} mm. Thus the movements of the walls of the supply and waste tubes, as well as of the pump section, are extremely small compared with their radii. The velocity of the wall is equal to the amplitude just calculated multiplied

by $\omega = 2\pi f_c$, where f_c is a characteristic frequency related to the action of the pump. Usually the ratio of the maximum wall velocity and the maximum velocity in the axial direction, which is related to the droplet velocity, remains very small, even for frequencies of the order of 1 MHz.

Using the relation (Landau & Lifshitz 1959)

$$c^2 = \frac{\partial p}{\partial \rho}, \tag{3}$$

and the estimate of the magnitude of the pressure waves, it appears that the variations of the density are of the order of 1 kg/m^3. Thus the variations of the density are extremely small compared with the value at rest (see data of figure 2). Moreover the length of the system is large compared with its cross-sectional dimensions. This is also true for most of the separate parts.

Guided by these remarks, we may expect that the fluid motion is mainly directed in the z-direction, and the gradients of the pressure and the density in the r-direction are negligible relative to the corresponding gradients in the z-direction. The lengths of the parts of the nozzle and the damper, however, are quite small. As long as the wavelengths of the pressure waves travelling through the system are long compared with the cross-sectional dimensions, the theory developed in the following also applies for these parts. When this is the case the influence of the compressibility of the fluid is small and the results of the calculation are similar to those for an incompressible viscous fluid. As usual, when dealing with incompressible viscous fluids, complex geometries such as the nozzle and the damper can be considered as a series of cylindrical tubes with different cross-sectional dimensions.

As the capillary pressures are very small compared with the magnitude of the pressure waves induced by charging the actuator, it will be assumed that at both ends of the pump the pressure inside the fluid is equal to the ambient pressure.

The following derivation applies to an element with radius R, length L, wall thickness h and Young's modulus E. In it moves a liquid with density ρ, velocity of sound c and viscosity μ. The velocity, density and pressure fields are defined with respect to a local cylindrical coordinate system (r, θ, z), the origin of which is at the entrance to the element.

Integration of the linearized equation of continuity (Landau & Lifshitz 1959),

$$\frac{\partial \rho}{\partial t} + \rho_0 \left\{ \frac{1}{r} \frac{\partial}{\partial r} (r v_r) + \frac{\partial v_z}{\partial z} \right\} = 0, \tag{4}$$

over the cross-section gives, after division by πR^2,

$$\frac{\partial \rho}{\partial t} + 2 \frac{\rho_0}{R} v_r|_{r=R} + \rho_0 \frac{\partial \bar{v}_z}{\partial z} = 0, \tag{5}$$

where

$$\bar{v}_z = \frac{1}{\pi R^2} \int_0^R 2\pi r v_z \, \mathrm{d}r. \tag{6}$$

The velocity v_r at the wall is given by

$$v_r|_{r=R} = \frac{(R + \frac{1}{2}h)^2}{Eh} \frac{\partial p}{\partial t} + \frac{\mathrm{d}f(t)}{\mathrm{d}t}. \tag{7}$$

The function $f(t)$ denotes the motion prescribed by the actuator ($f(t)$ is related to the applied voltage as mentioned: see the data of figure 2).

Inertia effects of the tube wall can be left out of account as long as the frequency of variations of $f(t)$ is small compared with the lowest eigenfrequency of the tube (see also (26) and (27)).

It is assumed that bending effects are negligible. This is allowed if the wavelengths of pressure waves are long compared with the cross-sectional dimensions of the element (Timoshenko & Woinowsky-Krieger 1959). Combination of the integrated equation of continuity (5) with the relations (3) and (7) results in

$$\frac{1}{\bar{c}^2}\frac{\partial p}{\partial t}+\rho_0\frac{\partial \bar{v}_z}{\partial z}+2\frac{\rho_0}{R}\frac{\mathrm{d}f(t)}{\mathrm{d}t}=0, \tag{8}$$

where

$$\frac{1}{\bar{c}^2}=\frac{1}{c^2}+2\frac{\rho_0}{R}\frac{(R+\frac{1}{2}h)^2}{Eh}. \tag{9}$$

The flow inside the tubular pump is characterized by a small value of the Strouhal number (Landau & Lifshitz 1959). The Strouhal number relates the convective momentum flux, associated with the bulk flow of fluid to the acceleration stresses. Consequently the convective terms in the equation of motion can be left out of account. Integration of the linearized equation of motion,

$$\rho_0\frac{\partial v_z}{\partial t}=-\frac{\partial p}{\partial z}+\mu\frac{1}{r}\frac{\partial}{\partial r}r\frac{\partial v_z}{\partial r}, \tag{10}$$

over the cross-section, and division by πR^2, yields

$$\rho_0\frac{\partial \bar{v}_z}{\partial t}=-\frac{\partial p}{\partial z}+2\mu\frac{1}{R}\frac{\partial v_z}{\partial r}\bigg|_{r=R}. \tag{11}$$

Elimination of $\bar{v}_z$ gives a set of two equations which describe approximately the non-stationary behaviour of a viscous and compressible liquid in a narrow long tube:

$$\frac{1}{\bar{c}^2}\frac{\partial^2 p}{\partial t^2}-\frac{\partial^2 p}{\partial z^2}+2\mu\frac{1}{R}\frac{\partial}{\partial z}\left(\frac{\partial v_z}{\partial r}\bigg|_{r=R}\right)+2\frac{\rho_0}{R}\frac{\mathrm{d}^2 f(t)}{\mathrm{d}t^2}=0, \tag{12a}$$

$$\rho_0\frac{\partial v_z}{\partial t}=-\frac{\partial p}{\partial z}+\mu\frac{1}{r}\frac{\partial}{\partial r}\left(r\frac{\partial v_z}{\partial r}\right). \tag{12b}$$

This set of equations is put in dimensionless form by introducing the folowing set of dimensionless quantities:

$$\left.\begin{aligned} &p^*=\frac{p}{p_0}\quad v_z^*=\frac{v_z}{v},\quad \tau=\omega t,\\ &r^*=r\left(\frac{\rho_0\omega}{\mu}\right)^{\frac{1}{2}},\quad z^*=\frac{z}{L},\quad f^*=\frac{f}{w_0},\\ &\alpha=\frac{\omega L}{\bar{c}},\quad \beta=\frac{\alpha}{\gamma}\frac{\bar{c}}{v}\frac{w_0}{R},\quad \gamma=\frac{p_0}{vL\rho_0\omega}. \end{aligned}\right\} \tag{13}$$

Substitution of (13) in (12) gives

$$\alpha^2\frac{\partial^2 p^*}{\partial\tau^2}-\frac{\partial^2 p^*}{\partial z^{*2}}+2\frac{1}{\gamma R^*}\frac{\partial}{\partial z^*}\left(\frac{\partial v_z^*}{\partial r^*}\bigg|_{r^*=R^*}\right)+2\beta\frac{\mathrm{d}^2 f^*(\tau)}{\mathrm{d}\tau^2}=0, \tag{14a}$$

$$\frac{\partial v_z^*}{\partial\tau}=-\gamma\frac{\partial p^*}{\partial z^*}+\frac{1}{r^*}\frac{\partial}{\partial r^*}\left(r^*\frac{\partial v_z^*}{\partial r^*}\right). \tag{14b}$$

We start with the solution of (14*b*) for v_z^*, such that the no-slip condition along $r^* = R^*$ and the symmetry condition along $r^* = 0$ are fulfilled. From the expression for v_z^* we calculate the derivative of v_z^* with respect to r^* at $r^* = R^*$ and substitute the result in (14*a*). In order to solve (14*a*) for the dimensionless pressure we must specify the function f. Equation (14) will be solved by the separation of variables. Suppose that

$$p^* = \mathrm{Re}\,(\hat{\pi}\,\mathrm{e}^{\mathrm{i}\tau}), \quad v_z^* = \mathrm{Re}\,(\hat{\phi}\,\mathrm{e}^{\mathrm{i}\tau}), \quad f^*(\tau) = \mathrm{Re}\,(\mathrm{e}^{\mathrm{i}\tau}). \tag{15}$$

The solution of (14*b*) that satisfies the boundary conditions mentioned is

$$v_z^* = -\mathrm{Re}\left[\gamma\,\mathrm{e}^{\mathrm{i}\tau}\frac{\partial\hat{\pi}}{\partial z^*}\left\{\frac{\mathrm{ber}\,r^*\,\mathrm{bei}\,R^* - \mathrm{bei}\,r^*\,\mathrm{ber}\,R^*}{\mathrm{ber}^2 R^* + \mathrm{bei}^2 R^*} + \mathrm{i}\left(\frac{\mathrm{bei}\,r^*\,\mathrm{bei}\,R^* + \mathrm{ber}\,r^*\,\mathrm{ber}\,R^*}{\mathrm{ber}^2 R^* + \mathrm{bei}^2 R^*} - 1\right)\right\}\right], \tag{16}$$

where $\mathrm{ber}\,r^*$ and $\mathrm{bei}\,r^*$ are Kelvin functions of zeroth order (Abramowitz & Stegun 1972).

The derivative of the dimensionless velocity at $r^* = R^*$ is

$$\left.\frac{\partial v_z^*}{\partial r^*}\right|_{r^*=R^*} = -\mathrm{Re}\left[\gamma\,\mathrm{e}^{\mathrm{i}\tau}\frac{\partial\hat{\pi}}{\partial z^*}(a_1 + \mathrm{i}a_2)\,R^*\right], \tag{17}$$

where

$$\left.\begin{aligned} a_1 &= \frac{1}{R^*}\,\frac{\mathrm{ber}\,R^*\,\mathrm{bei}'\,R^* - \mathrm{bei}\,R^*\,\mathrm{ber}'\,R^*}{\mathrm{ber}^2 R^* + \mathrm{bei}^2 R^*}, \\ a_2 &= \frac{1}{R^*}\,\frac{\mathrm{ber}\,R^*\,\mathrm{ber}'\,R^* + \mathrm{bei}\,R^*\,\mathrm{bei}'\,R^*}{\mathrm{ber}^2 R^* + \mathrm{bei}^2 R^*}, \end{aligned}\right\} \tag{18}$$

$\mathrm{ber}'\,R^*$ and $\mathrm{bei}'\,R^*$ are the first derivatives of $\mathrm{ber}\,r^*$ and $\mathrm{bei}\,r^*$ with respect to the argument at $r^* = R^*$ (Abramowitz & Stegun 1972). (Note that, apart from the division by R^*, a_1 and a_2 are quotients of cross-products of the Kelvin functions (Abramowitz & Stegun 1972).) Substitution of (15) and (18) in (14*a*) yields

$$\alpha^2\hat{\pi} + \frac{\partial^2\hat{\pi}}{\partial z^{*2}}(1 + 2a_1 + 2\mathrm{i}a_2) = -2\beta. \tag{19}$$

The solution for p^* is

$$p^* = \mathrm{Re}\left[\mathrm{e}^{\mathrm{i}\tau}\left\{(A\,\mathrm{e}^{-\alpha_1 z^*} + B\,\mathrm{e}^{\alpha_1 z^*})\cos\alpha_2 z^* + \mathrm{i}(A\,\mathrm{e}^{-\alpha_1 z^*} - B\,\mathrm{e}^{\alpha_1 z^*})\sin\alpha_2 z^* - 2\frac{\beta}{\alpha^2}\right\}\right], \tag{20}$$

where

$$\left.\begin{aligned} \alpha_1 &= \frac{\alpha}{(\mathrm{mod})^{\frac{1}{2}}}\sin\tfrac{1}{2}\theta, \\ \alpha_2 &= \frac{\alpha}{(\mathrm{mod})^{\frac{1}{2}}}\cos\tfrac{1}{2}\theta, \end{aligned}\right\} \tag{21}$$

and

$$\left.\begin{aligned} &\sin\theta = -\frac{2a_2}{\mathrm{mod}}, \quad \cos\theta = \frac{1 + 2a_1}{\mathrm{mod}}; \\ &\mathrm{mod} = \{(1 + 2a_1)^2 + 4a_2^2\}^{\frac{1}{2}}. \end{aligned}\right\} \tag{22}$$

After solving for p^*, the velocity v_z^* follows from (16).

Evaluation of (6) gives an expression of the mean velocity $\bar{v}_z^*$:

$$\bar{v}_z^* = -\mathrm{Re}\left[\gamma\,\mathrm{e}^{\mathrm{i}\tau}\frac{\partial\hat{\pi}}{\partial z^*}\{2a_2 - \mathrm{i}(2a_1 + 1)\}\right], \tag{23}$$

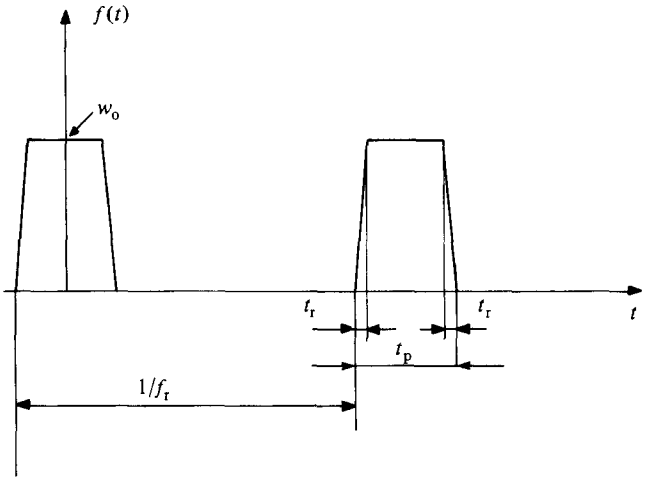

FIGURE 4. Series of trapezoidally shaped pulses, with pulse length t_p, rise-and-fall time t_r and repeat rate f_r.

where a_1 and a_2 are defined by (18). At present the solution contains two unknown complex constants A and B. These are found as follows. Let the tubular pump be divided into N parts. The total number of unknown complex constants is then $2N$. At the boundary of two elements we must ensure the continuity of pressure and mass flux; this provides $2(N-1)$ equations for the unknown constants. The remaining two are the constraints on the pressure at the ends of the pump, where it is assumed that the pressure inside the fluid is equal to the ambient pressure.

As the equations governing the fluid flow are linear, the response in the time domain can be found by Fourier analysis. We consider the case that the actuator is charged pulsewise at a constant rate of f_r pulses per second. The pulse shape is trapezoidal. The effect of such a pulse on the inside displacement of the corresponding part of the glass tube is depicted in figure 4.

The Fourier decomposition of such a series of pulses is

$$f(t) = w_0\left\{\tfrac{1}{2}\xi_0 + \mathrm{Re}\sum_{n=1}^{\infty}(\xi_n - \mathrm{i}\zeta_n)\,\mathrm{e}^{\mathrm{i}n\tau}\right\}, \tag{24}$$

where $\tau = \omega_r t$, $\omega_r = 2\pi f_r$, and the coefficients $\xi_0, \ldots, \xi_n, \ldots, \zeta_n, \ldots$ are

$$\left.\begin{aligned} \xi_0 &= \frac{\omega_r(t_p - t_r)}{\pi}, \quad \zeta_n = 0, \\ \xi_n &= -\frac{2}{\pi}\frac{1}{n^2\omega_r t_r}[\cos(\tfrac{1}{2}n\omega_r t_p) - \cos\{\tfrac{1}{2}n\omega_r(t_p - 2t_r)\}]. \end{aligned}\right\} \tag{25}$$

With use of the theory for $f(\tau) = \mathrm{Re}\,(\xi_n\,\mathrm{e}^{\mathrm{i}n\tau})$ $(n = 1, \ldots, \infty)$ the final result is found by adding up the outcomes for each n.

For the geometry given in figure 2 the response in the frequency domain is calculated. The division into parts is displayed in figure 3. Figure 5 shows the response of the fluid in the frequency domain in terms of the amplitude of the mean velocity at the end of the nozzle for the case that the amplitude of the actuator remains constant. Also displayed is the response of a system with a constriction at the beginning of the pump. The effect of a different viscosity on the fluid response is shown in figure 6.

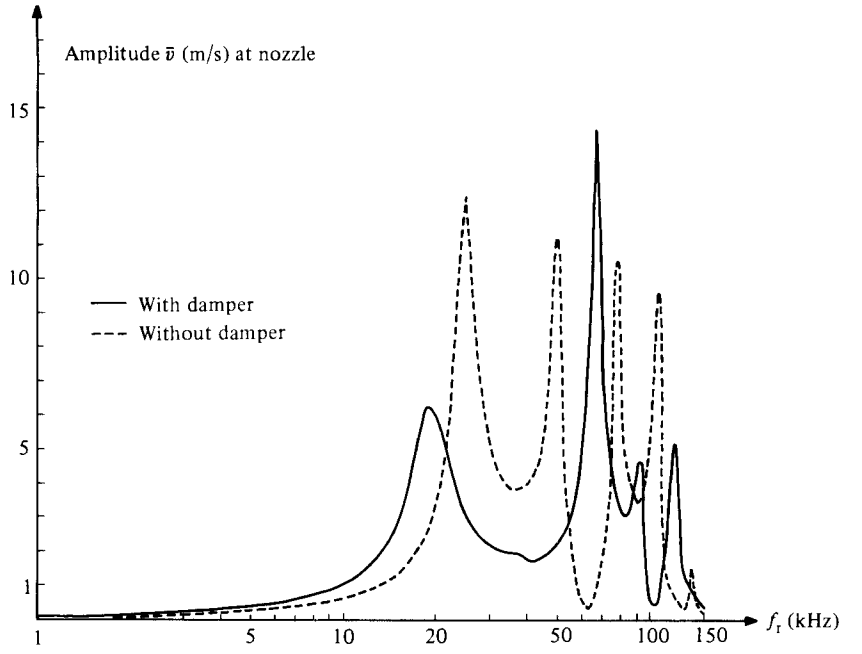

FIGURE 5. Responses of the fluid column in the frequency domain in terms of the amplitude of the mean velocity at the end of the nozzle for the system given in figure 2 with and without damper. The amplitude of the actuator is equal to 1.2×10^{-8} m.

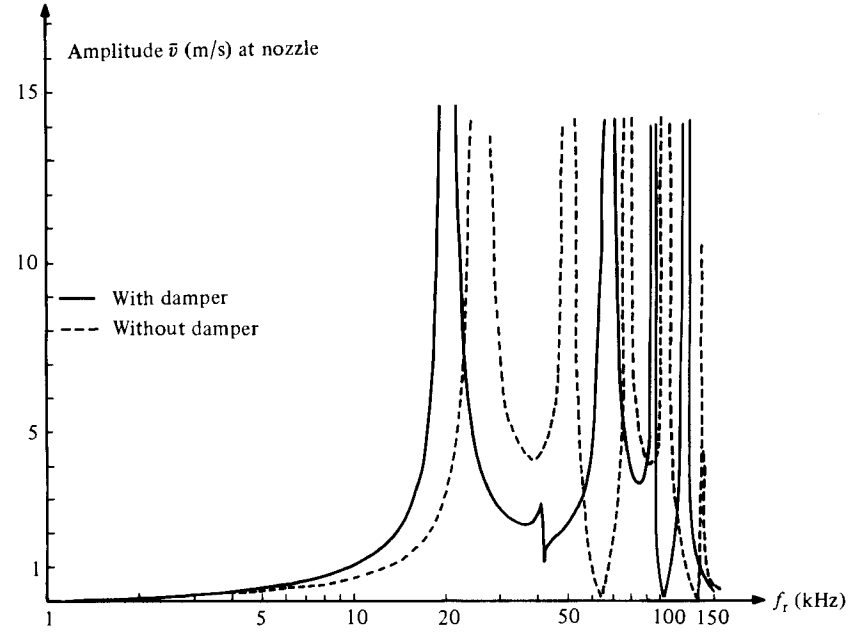

FIGURE 6. Responses of the same systems as used in figure 5, but with $\mu = 0.001$ Pa s.

When looking at the physical response of a system, we also observe some resonances coming from the structure of the pump. The most important one is the fundamental resonance of the piezoceramic actuator in the longitudinal direction:

$$f_{\text{piezo}} = \frac{1}{2L}\left(\frac{C_{11}^{\text{D}}}{\rho_{\text{piezo}}}\right)^{\frac{1}{2}}. \tag{26}$$

(According to Berlincourt *et al.* (1964), for PZT-5 it is found that $C_{11}^{\text{D}} = 1.26 \times 10^{11}$ Pa and $\rho_{\text{piezo}} = 7750$ kg/m^3. For the actuator considered f_{piezo} is roughly equal to 200 kHz.) Moreover, the longitudinal eigenmotions of the glass structure must be taken into account. For the case that the ends of the supply and waste tubes are not clamped stiffly in the writing head, an estimate of the fundamental resonances of these parts can be obtained by evaluation of

$$f_{\text{glass}} = \frac{1}{4L}\left(\frac{E}{\rho_{\text{glass}}}\right)^{\frac{1}{2}} \tag{27}$$

(Thompson 1966). As the mass of the piezoceramic actuator is large relative to that of the glass tube, it is assumed for the derivation of (27) that the glass tube is clamped in the actuator. (Inserting $E = 6.4 \times 10^{10}$ Pa and $\rho_{\text{glass}} = 2400$ kg/m^3, it is found that the fundamental resonances for the supply and waste tubes are 210 and 150 kHz respectively. When the system is filled with liquid these values are somewhat lower.)

Some results of the calculations in the time domain are given in figures 7 and 8. In order to obtain sufficient accuracy, the first 250 terms of the Fourier series (24) are used for all the calculations. Figure 7 shows the responses of the pump in the time domain expressed in terms of the mean velocity and the velocity for $r = 0$, both defined at the end of the nozzle, for pulses of different length. For the calculation the pump of figure 2 without damper is used. The displacement of the inside of the actuator is directed outwards during the pulse.

For the case $t_{\text{p}} = 18$ μs the velocity in the nozzle when it is positive for the first time is considerably higher than for the two other cases. This behaviour can be explained as follows.

A trapezoidal pulse consists of two equally shaped step functions with rise time t_{r} and opposite sign, which are supplied to the system with a delay time equal to $t_{\text{p}} - t_{\text{r}}$. During the first step the pressure is initially decreased in the pump section. At the ends of the pump section, pressure discontinuities are generated. Starting at these positions, two pressure-decreasing waves travel directly towards the nozzle and the reservoir, while two pressure-increasing ones travel through the pump section towards the nozzle and the reservoir. The pressure-decreasing wave from the end of the pump section reaches the nozzle first. The fluid in the nozzle sucks in. The pressure-increasing wave from the beginning of the pump section reaches the nozzle after travelling through the pump section and the waste tube and then starts eliminating the effect of the pressure-decreasing wave.

The pressure-decreasing wave in the supply tube is reflected at the open end as a pressure-increasing wave. When the second step is generated at the right moment, the reflected pressure-increasing wave and the pressure-increasing wave induced by the second step are added up in an optimal way.

Using this reasoning, an estimate of the optimal delay time can be obtained by calculating the time a pressure wave needs to travel twice through the supply tube and once through the pump section. From the definition of the pulse time (see figure 4) one must add to this result the rise time t_{r}. In the case discussed, using the

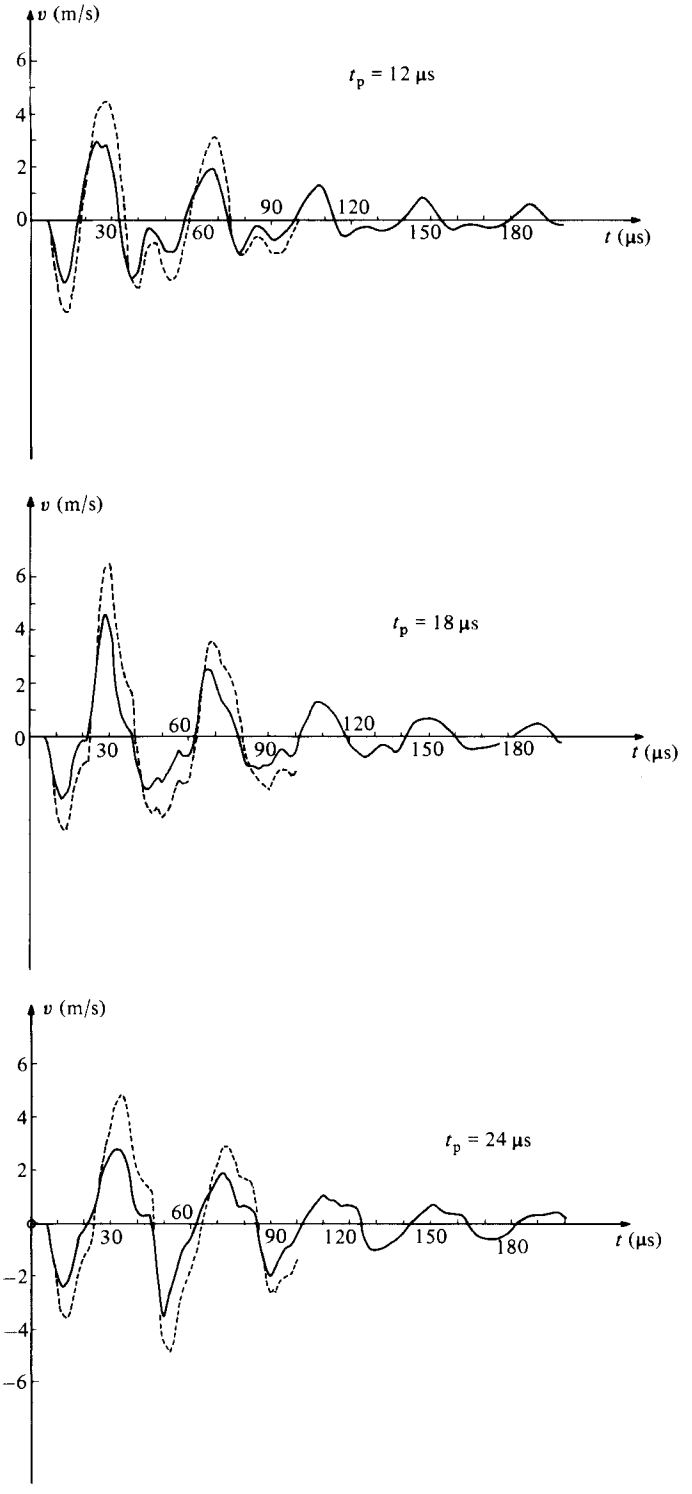

FIGURE 7. The responses in the time domain of the system given in figure 2 without damper in terms of the mean velocity and the velocity at $r = 0$, both defined at the end of the nozzle for three different pulse lengths. ——, mean velocity; ----, velocity at $r = 0$ (displayed during the first 100 μs). For each of the cases the rise time $t_r = 2$ μs, the repeat rate $f_r = 1000$ Hz and the pulse height $w_0 = 1.2 \times 10^{-8}$ m.

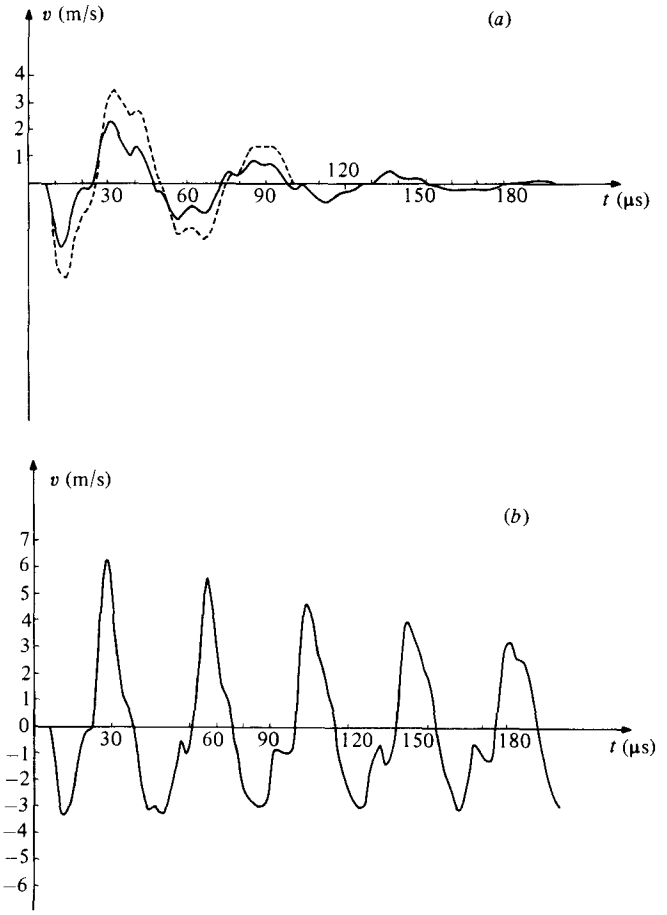

FIGURE 8. (*a*) The response of the system in figure 2 with damper. The pulse time is 18 μs, the rise time 2 μs, the repeat rate 1000 Hz and the pulse height 1.2×10^{-8} m. (*b*) The response of the system in figure 2 without damper, filled with a liquid whose viscosity μ is 0.001 Pa s ($t_p = 18$ μs, $t_r = 2$ μs, $f_r = 1000$ Hz and $w_0 = 1.2 \times 10^{-8}$ m).

appropriate values of the velocity of sound in the axial direction (9), it is found that $t_p = 18$ μs. For the optimal addition of the pressure-increasing waves it is essential that the beginning of the pump is open. The effect of a damper when the pump is operated with the same pulse is shown in figure 8(*a*). There is no amplification, since the pressure-decreasing wave starting from the beginning of the pump section towards the reservoir is reflected at the damper as a pressure-decreasing wave again. In figure 8(*b*) the effect of a much lower viscosity is elucidated for the system of figure 2 without damper. It is remarkable that in the low-viscosity case the difference between the mean velocity and the velocity at $r = 0$ has nearly disappeared.

The extent of coupling of (14*a*) with (14*b*) depends on the magnitude of R^*. With constant dimensions and density of the fluid, this coupling decreases with decreasing viscosity. The influence of the viscosity in a pulsating flow depends on the ratio of the Strouhal number S and the Reynolds number R:

$$\frac{S}{R} = \frac{\mu t_c}{\rho_0 R^2}. \tag{28}$$

A reasonable guess for t_c is $t_c = L/c$, where L is the overall length of the system. Inserting the data of, for example, the structure given in figure 2, it appears that in this case the number defined by (28) is small, except in the nozzle, where it reaches a value of order unity. In the case considered in figure 8(*b*) this number is small to extremely small everywhere, and the fluid behaves nearly as an inviscid liquid.

3. Droplet formation

Droplet formation is a phenomenon that depends on the viscosity and surface tension of the liquid and on the velocity distribution in the nozzle as a function of time and space. The actual droplet formation is very complicated indeed. (For a series of photographs showing successive stages of droplet formation see figure 9 (Döring 1982).) We will present here a strongly simplified method, which, however, predicts the droplet radius and its velocity quite well, without going into details about precisely what happens at the end of the nozzle.

The description is based on the following assumptions.

(1) Basically the droplet formation depends on the ratio of the kinetic energy transported outwards to the energy needed to form the surface of the droplet. If this number is larger than unity, then in principle a droplet can be formed. Among other things the velocity of the droplet depends on the amount by which this ratio exceeds unity. The viscosity does not play any direct role in the exchange of energies. Indirectly there will be an effect since the velocity distribution in the nozzle depends on the viscosity.

(2) The influence of the ambient air will be neglected. This statement can be checked as follows. The drag force exerted by the air on a droplet with radius R_d is expressed by the formula (Bird, Stewart & Lightfoot 1960)

$$F = \pi R_d^2 \times \tfrac{1}{2}\rho v_d^2 f, \tag{29}$$

where the friction factor f depends on the Reynolds number $\mathbb{R}$ appropriate to this case

$$\mathbb{R} = \frac{2\rho_{air} v_d R_d}{\mu_{air}}, \tag{30}$$

and by the modified Stokes law

$$f = 1.85\mathbb{R}^{-\frac{1}{3}} \quad (2 < \mathbb{R} < 500). \tag{31}$$

Then the deceleration of the droplet due to air friction equals

$$\frac{dv_d}{dt} = -\tfrac{3}{8} f \frac{\rho_{air}}{\rho_{fluid}} \frac{v_d^2}{R_d}. \tag{32}$$

(After inserting $\rho_{air} = 1.2$ kg/m^3, $v_d = 3$ m/s, $R_d = 0.05$ mm and

$$\mu_{air} = 1.85 \times 10^{-5}\,\text{Pa s} \quad (T = 20\ ^\circ\text{C}),$$

the deceleration is found to be about -240 m/s^2. When we look at a point a distance of 1 mm away from the nozzle, which is quite a large distance compared with the droplet dimensions, the velocity is lowered by an amount of 0.1 m/s.)

(3) The time during which the velocity in the nozzle is positive is so short that no long jets will be formed. A long jet has a length of at least several times the diameter of the nozzle (Weber 1931).

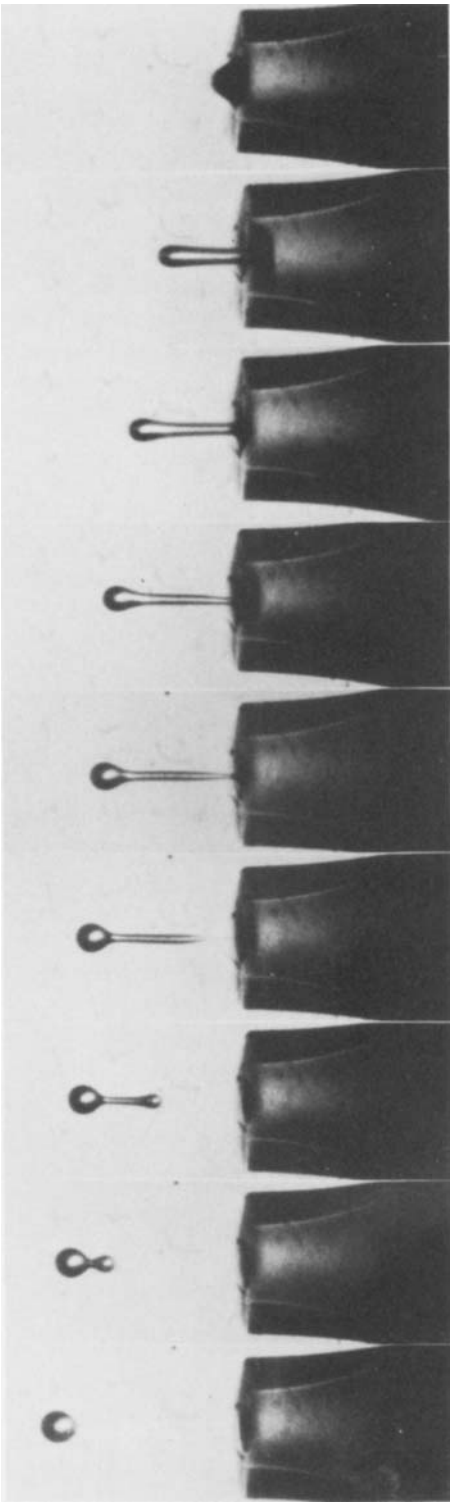

FIGURE 9. A series of photographs showing successive stages of droplet formation. (Photographs reproduced by kind permission of the author from Döring (1982).)

At time $t = t_1$ the mean velocity and the velocity at $r = 0$, both defined at the end of the nozzle, have changed sign from negative to positive. At that time we define a control volume just in front of the fluid–air interface. For $t > t_1$ a certain amount of fluid and kinetic energy will be transferred through the surface of the control volume. The volume $V(t)$ that has passed the control-volume surface is

$$V(t) = \pi R_n^2 \int_{t_1}^{t} \bar{v}_z \, dt', \tag{33}$$

where R_n is the radius of the nozzle.

A viscous fluid transports twice the amount of kinetic energy as an inviscid fluid does, provided that the mean velocity in both cases is identical. To incorporate this effect, the amount of kinetic energy transported through the surface of the control volume is approximated by

$$T(t) = \tfrac{1}{2}\pi\rho R_n^2 \int_{t_1}^{t} \bar{v}_z^2 v_z|_{r=0} \, dt'. \tag{34}$$

Note that for the inviscid case and the purely viscous case the expression for $T(t)$ is exact. In other cases it is an approximation.

As the droplet formation basically consists of the conversion of kinetic energy into surface energy, the enlargement of the free surface must be calculated. In order to do this we assume that initially the shape of the fluid portion inside the control volume is a body of revolution, the generator of which is given by

$$F(r, t) = \int_{t_1}^{t} v_z(r, t') \, dt'. \tag{35}$$

$F(r, t)$ is defined with respect to the surface of the control volume just before the nozzle, which is supposed to be flat at that place. In fact (35) expresses that the emerging fluid is modelled as flowing in discrete concentric cylindrical shells, like an expanding telescope. Then the enlargement of the free surface can be found by evaluation of

$$\mathcal{O}(t) = 2\pi \int_0^{R_n} r\left[1 + \left(\frac{\partial F(r, t)}{\partial r}\right)^2\right]^{\frac{1}{2}} dr - \pi R_n^2. \tag{36}$$

For the inviscid case we have

$$\mathcal{O}(t) = 2\pi R_n \int_{t_1}^{t} \bar{v}_z \, dt' = \pi R_n^2 \lambda, \tag{37}$$

where λ is defined as the ratio of twice the integral of the mean velocity over the time interval considered to the radius R_n of the nozzle. For the purely viscous case at any instant the velocity profile is a parabolic function of r. On using this, evaluation of (36) yields

$$\mathcal{O}(t) = \pi R_n^2 \left[\frac{1}{6\lambda^2}\{(1 + 4\lambda^2)^{\frac{3}{2}} - 1\} - 1\right]. \tag{38}$$

The kinetic energy $T(t)$ is needed to enlarge the free surface. In the beginning the difference between $T(t)$ and $\sigma\mathcal{O}(t)$, where σ is the surface tension, is negative. Let us assume that at a certain time t_2 the situation is reached for which

$$T(t_2) - \sigma\mathcal{O}(t_2) = 2\pi \int_0^{R_n} \tfrac{1}{2}\rho F(r, t_2) \, r v_z^2(r, t_2) \, dr. \tag{39}$$

At that instant the kinetic energy of the fluid portion inside the control volume is just equal to the difference of the kinetic energy transported through the surface of the control volume during $t_1 < t < t_2$ and the energy needed to enlarge the free surface. Using the same reasoning as for the derivation of (34), we obtain

$$T(t_2) - \sigma \mathcal{O}(t_2) = \tfrac{1}{2}\rho V(t_2)\, \bar{v}_z(t_2)\, v_z(t_2)|_{r=0}. \tag{40}$$

On evaluating (40), it appears that this condition can be fulfilled only if

$$\int_{t_1}^{t} \bar{v}_z(t')\{\bar{v}_z(t')|_{r=0} - \bar{v}_z(t_2)\, v_z(t_2)|_{r=0}\}\, \mathrm{d}t' > 0, \tag{41}$$

which means that the velocity in the nozzle has gone through a maximum before the situation given by (40) is reached. Together with the fact that the droplet velocity must be as high as several metres per second, this leads to the conclusion that the value of λ at the moment that a droplet can be formed is at least of order unity. Then expression (38) can be approximated by

$$\mathcal{O}(t) \approx \pi R_n^2 \left(\frac{4\lambda}{3} + \frac{1}{2\lambda} - \frac{1}{6\lambda^2} - 1\right) \quad (\lambda \geqslant 1). \tag{42}$$

In order to determine $\mathcal{O}(t)$ for intermediate cases we use

$$\mathcal{O}(t) \approx \pi R_n^2 \left\{ \lambda + \left(\frac{\int_t^{t_1} v_z|_{r=0}\, \mathrm{d}t'}{\int_t^{t_1} \bar{v}_z\, \mathrm{d}t'} - 1 \right) \left(\tfrac{1}{3}\lambda + \frac{1}{2\lambda} - \frac{1}{6\lambda^2} - 1 \right) \right\}. \tag{43}$$

The term in parentheses containing the integrals of the velocity at $r = 0$ and the mean velocity can be considered as a measure of the extent to which viscous effects will dominate. Equation (43) is an approximation, which is valid only for the limiting cases discussed. When the velocity decreases at $t > t_2$ the volume $V(t_2)$ will be the future droplet volume V_d. Before the droplet is released for a short time, it is connected to the fluid in the nozzle by a stretching fluid thread (see figure 9). The creation of a free surface during stretching is simply taken into account by stating that the separation of the droplet from the fluid in the nozzle implies the generation of two surfaces equal to $\pi R_n^2\, \bar{v}_z(t_2)/v_z(t_2)|_{r=0}$. One surface belongs to the droplet, the other one to the fluid in the nozzle. Using this, and for the time being leaving out of account the influence of viscosity during stretching, the droplet velocity is found to be

$$v_d = \left[\bar{v}_z(t_2)\, v_z(t_2)|_{r=0} - \frac{2\pi\sigma R_n^2\, \bar{v}_z(t_2)}{\rho V_d\, v_z(t_2)|_{r=0}} \right]^{\frac{1}{2}}, \tag{44}$$

provided that the argument of the square root is positive, otherwise no droplet will be launched. In order to investigate the possibility of forming more droplets at $t > t_2$, the analysis must be continued with

$$\mathcal{O}(t_2) = V(t_2) = 0, \quad T(t_2) = -\sigma\pi R_n^2 \frac{\bar{v}_z(t_2)}{v_z(t_2)|_{r=0}} \quad (t > t_2). \tag{45}$$

An estimate of the influence of the elongational viscosity, which is three times the dynamic viscosity (Petrie 1979), on the droplet velocity can be obtained as follows.

At time $t = t_2$ the tip of the fluid has reached the position

$$F(0, t_2) = \int_{t_1}^{t_2} v_z|_{r=0}\, \mathrm{d}t'. \tag{46}$$

In order to simplify the calculation we assume the following.

(1) At $t = t_2$ the shape of the fluid portion inside the control volume is replaced by a cylinder, the radius $R_j(t_2)$ of which is given by

$$\pi R_j^2(t_2)\, L_j(t_2) = V_d, \tag{47}$$

where $L_j(t_2) = F(0, t_2)$. During stretching, there is an increase in the length of the cylinder $L_j(t)$ and a decrease of the radius $R_j(t)$, such that condition (47) still holds good, t_2 being replaced by t.

(2) The total mass of the jet is concentrated in the tip of the jet. The velocity of the tip will be related to the droplet velocity.

(3) The interface of the stretching jet and the fluid inside the nozzle moves with a velocity equal to $\bar{v}_z$.

For $t > t_2$ the deceleration of the tip of the jet is given by

$$\rho V_d \frac{dv_d}{dt} = -3\mu \frac{v_d(t) - \bar{v}_z(t)}{L_j(t)} \pi R_j^2(t). \tag{48}$$

On using (47) and keeping in mind that $v_d(t) - \bar{v}_z(t)$ equals the time rate of change of the length of the jet, we arrive at

$$\frac{dv_d}{dt} = -\frac{3\mu}{\rho} \frac{1}{[L_j(t)]^2} \frac{dL_j(t)}{dt}. \tag{49}$$

An approximate solution for this differential equation reads

$$\Delta v_d = -\frac{3\mu}{\rho} \frac{1}{L_j(t_2)}. \tag{50}$$

To arrive at this approximate result it is supposed that the fluid filament becomes fairly long before it breaks. In that case the initial length, which is equal to $L_j(t_2)$, is the determining parameter.

Figure 10 shows the droplet velocity as a function of the pulse length and pulse height. One set of curves is calculated with the aid of (44), the second with the correction (50). It is clear that the influence of the viscosity on the droplet velocity is very significant. Therefore in the following the correction term defined by (50) is used all the time. Figure 11 displays the droplet velocity as a function of the repeat rate f_r. Above 3 kHz the influence of the poor damping of the fluid inside the pump is clearly depicted. Also shown is an experimental curve found with a pump very similar to the one used for the calculations. (The experimental curve was obtained at Philips' Research Laboratories in Hamburg by W. Ratke.)

Figure 12 (*a*) gives an overview of the influence of the viscosity on the droplet size, droplet speed and the frequency up to which the deviations of droplet velocity are smaller than 0.2 m/s. This frequency is used as a measure for the damping. All the other system parameters are kept constant. A low viscosity results in a higher droplet velocity. The damping, however, is worse. Increasing the viscosity improves the damping but lowers the droplet velocity. Above a certain value no droplet will be launched any more.

From figure 12 (*a*) we can estimate the temperature sensitivity of the pump system. The dependence of the viscosity on temperature can be expressed as

$$\mu(T) = \mu(T_0)\, e^{-b(T - T_0)}, \tag{51}$$

provided that T is in the neighbourhood of T_0 (Winter 1977). The value of the coefficient b is almost the same for different fluids. Consequently, for a certain

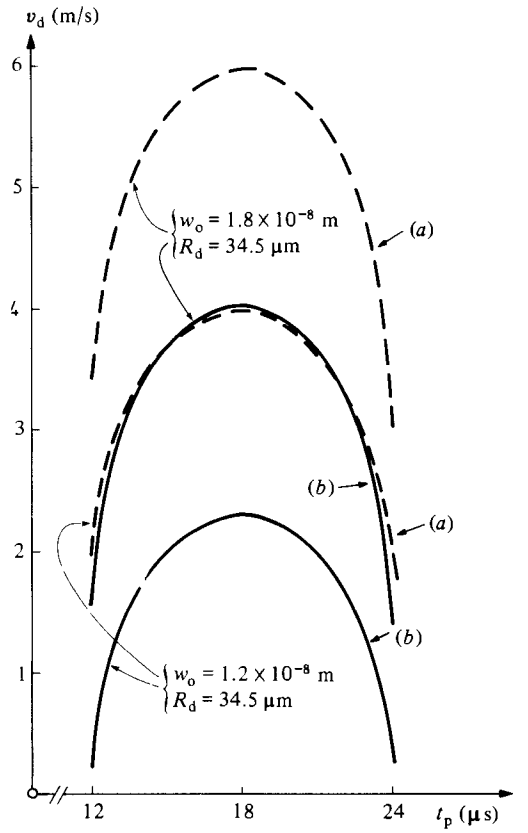

FIGURE 10. The droplet velocity as a function of the pulse length and pulse height. The droplets are generated with the pump of figure 2 without damper. For all the cases $t_r = 2$ μs and $f_r = 1000$ Hz. The dashed curves refer to results obtained with (44). Curves (*b*) were calculated with the aid of (44) and (50). (System of figure 2 without damper.)

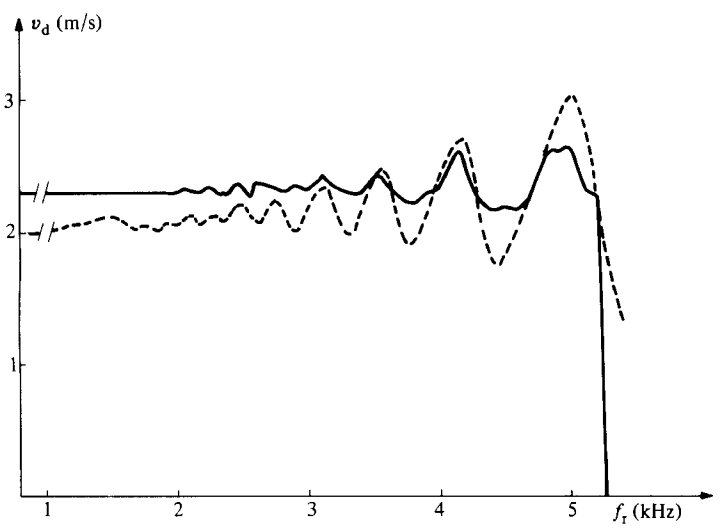

FIGURE 11. The droplet velocity as a function of the repeat rate f_r. (System of figure 2 without damper.) The solid line refers to the analytical results, the dashed line to experimental data, found for a very similar system. (The experiments were done at Philips' Research Laboratories in Hamburg by W. Ratke.)

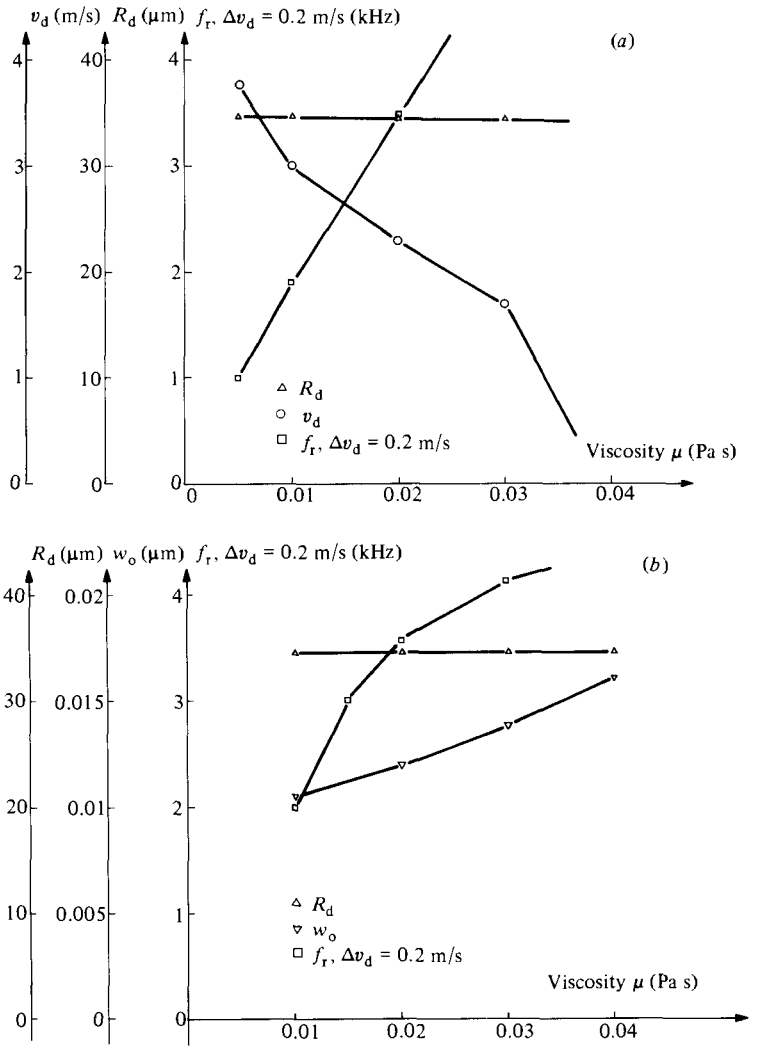

FIGURE 12. (*a*) The droplet velocity, droplet size and the frequency above which the deviations of the droplet velocity becomes larger than 0.2 m/s, displayed as functions of the viscosity. (System of figure 2 without damper, $t_p = 18$ μs, $t_r = 2$ μs, $f_r = 1000$ Hz, $w_0 = 1.2 \times 10^{-8}$ m.) (*b*) The droplet size, amplitude w_0 and the frequency above which the deviations of the droplet velocity becomes larger than 0.2 m/s for the case of constant droplet velocity displayed as functions of the viscosity. (System of figure 2 without damper, $t_p = 18$ μs, $t_r = 2$ μs, $f_r = 1000$ Hz, $v_d = 2.3$ m/s.)

temperature step the change of the viscosity is proportional to $\mu(T_0)$. As the droplet velocity is nearly a linear function of the viscosity we may conclude that the droplet velocity of a highly viscous fluid is more sensitive to temperature than a low-viscosity fluid.

Figure 12(*b*) gives an overview of the influence of the viscosity on the droplet size, the pulse height w_0 and the damping for the case of constant droplet velocity. We see that in order to obtain a better damping the fluid must be more viscous, which requires a higher voltage necessary to activate the pump. However, improved damping can only be achieved at the expense of increased temperature sensitivity. Thus the choice of the viscosity is necessarily a compromise.

REFERENCES

ABRAMOWITZ, M. & STEGUN, I. A. 1972 *Handbook of Mathematical Functions.* Dover.
BERLINCOURT, D. A., CURRAN, D. R. & JAFFE, H. 1964 *Physical Acoustics I*, part A, chap. 3.
BIRD, R. B., STEWART, W. E. & LIGHTFOOT, E. N. 1960 *Transport Phenomena.* Wiley.
DÖRING, M. 1982 *Philips Tech. Rev.* **40** (7), 192–198.
LANDAU, L. D. & LIFSHITZ, E. M. 1959 *Fluid Mechanics.* Pergamon.
PETRIE, C. J. S. 1979 *Elongational Flows.* Pitman.
PHILIPS Application Handbook 1974 *Piezoelectric Ceramics.* Mullard.
THOMSON, W. T. 1966 *Vibration Theory and Applications.* George Allen & Unwin.
TIMOSHENKO, S. P. & WOINOWSKY-KRIEGER, S. 1959 *Plates and Shells.* McGraw-Hill.
WEAST, R. C. (ed.) 1974 *Handbook of Chemistry and Physics.* CRC Press.
WEBER, C. 1931 *Z. angew. Math. Mech.* **11**, 136–154.
WINTER, H. H. 1977 *Adv. Heat Transfer*, pp. 205–268.